Substrate and Cofactor Reactivity of a Carbon Monoxide Dehydrogenase–Corrinoid Enzyme Complex: Stepwise Reduction of Iron–Sulfur and Corrinoid Centers, the Corrinoid $Co^{2+/1+}$ Redox Midpoint Potential, and Overall Synthesis of Acetyl-CoA†

David A. Grahame

Department of Biochemistry, Uniformed Services University of the Health Sciences, 4301 Jones Bridge Road, Bethesda, Maryland 20814-4799

Received April 27, 1993; Revised Manuscript Received July 7, 1993®

ABSTRACT: Cleavage of the acetyl carbon–carbon bond of acetyl-CoA in *Methanosarcina barkeri* is catalyzed by a high molecular mass multienzyme complex. The complex contains a corrinoid protein and carbon monoxide dehydrogenase and requires tetrahydrosarcinapterin (H_4SPt) as methyl group acceptor. Reactions of the enzyme complex with carbon monoxide and with the methyl group donor N^5-methyltetrahydrosarcinapterin (CH_3-H_4SPt) have been analyzed by UV-visible spectroscopy. Reduction of the enzyme complex by CO occurred in two steps. In the first step, difference spectra exhibited peaks of maximal absorbance decrease at 426 nm (major) and 324 nm (minor), characteristic of Fe-S cluster reduction. In the second step, corrinoid reduction to the Co^{1+} level was indicated by a prominent peak of increased absorbance at 394 nm. Spectrophotometric analyses of the corrinoid redox state were performed on the intact complex at potentials poised by equilibration with gas mixtures containing different $[CO_2]/[CO]$ ratios or by variation of the $[H^+]/[H_2]$ ratio. The corrinoid $Co^{2+/1+}$ midpoint potential was −426 mV (±4 mV, $n = 1.16$ electrons, 24 °C), independent of pH (pH 6.4–8.0). The results indicated a significant fraction of Co^{1+} corrinoid at potentials existing *in vivo*. The reduced corrinoid reacted very rapidly with CH_3-H_4SPt. Reaction with methyl iodide was slow, and methylation by *S*-adenosylmethionine was not observed. The rate of methyl group transfer from CH_3-H_4SPt greatly exceeded the rate of CO reduction of enzyme centers. The enzyme complex catalyzed efficient synthesis of acetyl-CoA from coenzyme A, CO, and CH_3-H_4SPt. During acetyl-CoA synthesis, demethylation of CH_3-H_4SPt was monitored by the absorbance increase at 312 nm. Concomitant appearance of the 394-nm enzyme peak indicated Co^{1+} corrinoid regeneration from Co^{3+}-methyl corrinoid. Results support the proposed function of the corrinoid as methyl group carrier during acetyl-CoA synthesis and decomposition.

The metalloenzyme carbon monoxide dehydrogenase (CODH)[1] plays a central metabolic role in acetyl-CoA synthesis and decomposition in a number of chemolithoautotrophic organisms. The enzyme contains nickel, and nonheme iron in Fe-S clusters, and catalyzes reversible assembly and disassembly of the acetyl moiety of acetyl-CoA from two separate one-carbon precursors. CODH also catalyzes redox interconversion of CO_2 and CO. Moreover, CO acts efficiently as a carbonyl group precursor substrate supporting net synthesis of acetyl-CoA in enzymic reaction mixtures that are reasonably well-defined (Hu et al., 1982; Pezacka & Wood, 1986, 1988; Abbanat & Ferry, 1990; Lu et al., 1990; Roberts et al., 1992).

Studies on the function, structure, and mechanism of action of CODH and other proteins involved in acetyl-CoA synthesis have been advanced farthest using the acetogenic organism *Clostridium thermoaceticum* [for reviews, see: Wood et al. (1986), Ljungdahl (1986), Ragsdale et al. (1988), and Ragsdale (1991)]. Although the enzymic mechanisms lack detail, recent review articles by Ferry (Ferry, 1992a,b) recount that significant progress is being made in studies of acetyl-CoA cleavage in methanogens.

The most critical piece of mechanistic information about how acetyl-CoA assembly takes place was obtained by Ragsdale and Wood, who discovered that CODH also catalyzes isotopic exchange of the carbonyl group of acetyl-CoA with carbon monoxide (Ragsdale & Wood, 1985). For carbonyl group exchange to occur, both the carbon–carbon bond (between C1 and C2) and the thioester bond of acetyl-CoA must undergo breakage and reformation. The CO-exchange reaction was diagnostic for the capacity of the enzyme to catalyze both insertion and excision of the carbonyl group of acetyl-CoA.

In *C. thermoaceticum*, a methylated 88-kDa corrinoid/iron–sulfur protein serves as proximal source of the methyl moiety for acetyl-CoA assembly on CO dehydrogenase. The corrinoid/iron–sulfur protein is required for net synthesis of acetyl-CoA with methyl iodide as precursor of the acetyl-CoA methyl moiety (Lu et al., 1990). Mössbauer and EPR studies demonstrated that the corrinoid/iron–sulfur protein contains a $[4Fe\text{-}4S]^{2+/1+}$ center (Ragsdale et al., 1987). The corrinoid cofactor was identified as 5-methoxybenzimida-

† The opinions or assertions contained herein are the authors' and are not to be construed as official or reflecting the views of the U.S. Department of Defense or the Uniformed Services University of the Health Sciences.

® Abstract published in *Advance ACS Abstracts,* September 15, 1993.

[1] Abbreviations: CODH, carbon monoxide dehydrogenase; EPR, electron paramagnetic resonance; NHE, normal hydrogen electrode; H_4SPt, tetrahydrosarcinapterin; CH_3-H_4SPt, N^5-methyltetrahydrosarcinapterin; E_0', standard reduction potential at pH 7; MOPS, 3-(*N*-morpholino)propanesulfonic acid, sodium salt; MES, 2-(*N*-morpholino)ethanesulfonic acid, sodium salt; AdoMet, *S*-adenosylmethionine; TRIQUAT, *N,N'*-trimethylene-2,2'-dipyridinium dibromide (E_0' of −540 mV); *R*, gas constant (1.987 cal mol^{-1} K^{-1}); *T*, absolute temperature (K); *F*, Faraday constant (23 063 cal V^{-1} $equiv^{-1}$).

This article not subject to U.S. Copyright. Published 1993 by the American Chemical Society

zolylcobamide. The isolated protein contained the cobamide cofactor in the Co^{2+} valence state, with the base, 5-methoxybenzimidazole, not involved in coordination to cobalt ("base-off" form). Electronic absorption spectra of the methylated corrinoid also indicated base-off Co^{3+}-methyl corrinoid. Potentiometric studies, in which the Co^{2+} oxidation state was quantified by EPR spectroscopy, indicated that E_0' of the $Co^{2+/1+}$ protein-bound corrinoid was −504 mV (NHE) (Harder et al., 1989). This value of E_0' is approximately 106 mV more positive than that found for free cobalamin or than would be expected for the free coenzyme $Co^{2+/1+}$ couple. It was concluded that a major factor contributing to the increased stability of the nucleophilic Co^{1+} state was the base-off configuration of the corrinoid.

In methanogenic bacteria CO dehydrogenase and a corrinoid protein are present together as components of a high molecular mass multienzyme complex composed of five distinct subunits in approximately equimolar amounts (Terlesky et al., 1986; Grahame, 1991). Although independent methods are needed to firmly establish the native molecular mass, the mass of the *Methanosarcina barkeri* complex was estimated to be 1.6 MDa by HPLC gel filtration (Grahame, 1991). Quantitative analyses indicate one corrinoid cofactor present per heteropentameric unit (Abbanat & Ferry, 1991; Grahame, 1991). The *Methanosarcina thermophila* enzyme complex catalyzes isotopic exchange of the carbonyl group of acetyl-CoA with CO at a rate that is slow compared with the same reaction catalyzed by CODH from *C. thermoaceticum* (Raybuck et al., 1991). Net cleavage of acetyl-CoA was demonstrated using the enzyme complex isolated from acetate-grown *M. barkeri* (Grahame, 1991).

The methyl group acceptor tetrahydrosarcinapterin (H_4SPt) was required for net cleavage of acetyl-CoA (Grahame, 1991). In overall cleavage of acetyl-CoA, the carbonyl group is oxidized to CO_2, and the methyl group is transferred to H_4SPt (a tetrahydrofolate analog). Evidence was obtained for the indicated stoichiometry, and a balanced equation for net cleavage of acetyl-CoA was formulated as follows:

$$CH_3CO\text{-}SCoA + H_4SPt + H_2O \rightarrow$$
$$HS\text{-}CoA + CH_3\text{-}H_4SPt + CO_2 + 2H^+ + 2e^- \quad (1)$$

Spectrophotometric measurements showed that during cleavage of acetyl-CoA reducing equivalents were generated, causing reduction of Fe-S centers in the enzyme complex.

In this report, spectrophotometric evidence was acquired indicating a sequential process of reduction of Fe-S and corrinoid centers in the multienzyme complex from *M. barkeri*. The apparent $Co^{2+/1+}$ redox midpoint potential of the enzyme-bound corrinoid cofactor was established, and efficient catalysis of acetyl-CoA synthesis was demonstrated. The findings support the proposal of a high redox potential corrinoid protein as an intermediate carrier of the methyl group during acetyl-CoA synthesis and cleavage.

MATERIALS AND METHODS

Reagents. Coenzyme A, disodium salt, >96% (HPLC), was purchased from Fluka Chemical Corp. Tetrahydrosarcinapterin (H_4SPt) and N^5-methyltetrahydrosarcinapterin (CH_3-H_4SPt) were produced as described previously (Grahame, 1991). Hydrogen gas was humidified and purified by bubbling through a gas-washing apparatus containing a solution of reduced methyl viologen. The solution (1 mM methyl viologen, 50 mM EDTA, and 100 mM Tris·HCl, pH 8) was reduced by addition of a slight excess of $TiCl_3$. High-purity argon was obtained from Union Carbide, Linde Corp. (Argon Zero, O_2 < 0.5 ppm). Except when used for pressurization of ultrafiltration equipment, argon gas was humidified and purified by the same procedure used for hydrogen. Carbon dioxide was likewise washed except that 0.5 M sodium bicarbonate was added to the reduced methyl viologen solution. Carbon monoxide gas was obtained from the same source as described earlier (Grahame & Stadtman, 1987). Carbon monoxide was introduced into reaction mixtures by addition of an aliquot of water saturated with CO at approximately 23 °C. From the α-value of 0.02208 (Lange, 1969) for CO solubility in water at 23 °C, saturated CO was calculated to be 0.986 mM. Spectrophotometric measurements were made using a Hewlett-Packard 8452A diode array UV-visible spectrophotometer. Spectral analyses employed the Quant II multicomponent analysis software on an associated HP ChemStation computer. Corrinoid analyses were performed as previously described (Grahame, 1991). All reactions and final preparations of reagents and gases were carried out inside the Anaerobic Laboratory at the National Institutes of Health (Poston et al., 1971).

CODH–Corrinoid Enzyme Complex. CO dehydrogenase–corrinoid complex was isolated from acetate-grown *M. barkeri* by anaerobic gel filtration on Sepharose CL-6B-200 as previously described (Grahame, 1991). Protein was measured by the dye-binding method of Bradford (Bradford, 1976). The CODH specific activity was approximately 40 units/mg [assayed by method a of Grahame and Stadtman (1987)]. SDS–gel electrophoresis revealed five major bands belonging to the enzyme complex and several minor bands. On the basis of densitometric analyses, none of the minor bands exceeded 3% of the total protein. Analyses of corrinoid indicated 0.86 mol of the cofactor per 271 800 g of protein (Grahame, 1991). Further purification employed stepwise elution from phenyl-Sepharose 4B (Pharmacia) as follows: A 5-mL sample (approx. 24 μM corrinoid) of the pooled and concentrated enzyme complex obtained from gel filtration was removed from storage and thawed under argon. After addition of an equal volume of an argon-saturated solution containing 1.0 M sodium sulfate, 50 mM sodium 3-(*N*-morpholino)propanesulfonate (MOPS), and 20 mM EDTA, pH 7.6, the solution was applied to a column (1.5-cm diameter, approx. 8.8-mL bed volume) of phenyl-Sepharose 4B, previously equilibrated with a solution (1× phenyl solution) consisting of 0.5 M Na_2SO_4, 25 mM MOPS, and 10 mM EDTA, pH 7.3, saturated with argon. The column was washed with 24 mL of 1× phenyl solution. After 4 mL of the enzyme solution had been applied, three effluent fractions (approx. 12 mL each) were collected. The first effluent fraction was turbid and slightly yellow in color. It contained less than 2% of the original CODH activity, but about half of the original hydrogenase activity (benzyl viologen reducing). The second and third fractions were colorless and clear. The enzyme complex was eluted in 2-mL fractions with 10 mM MOPS and 5 mM EDTA, pH 7.2. Fractions 2–9 were pooled and concentrated by ultrafiltration in a stirred cell under argon on an Amicon YM-30 membrane. The concentrate (1.5 mL, 53 μM corrinoid) was frozen dropwise in liquid nitrogen for storage. The yield was 66% of the original enzyme complex (based on corrinoid content), with only 10% of the original hydrogenase activity remaining. In assays of the thawed material for overall acetyl-CoA cleavage using the method described previously (Grahame, 1991) a lag period of about 10 min was observed. The lag period was completely eliminated by a 15-min preincubation of the enzyme with 20 μM CO prior to the assay. Maximal specific activity of acetyl-

CoA cleavage was not changed by chromatography on phenyl-Sepharose.

Corrinoid and Fe/S Spectral Components. Spectra were recorded at 10-s intervals throughout the time course of reduction of the enzyme complex at 36 °C in a 0.60-mL reaction mixture containing 1.6 nmol of enzyme corrinoid and 12 nmol of CO. Changes in the shape of difference spectra were monitored as a function of time by subtracting each subsequent spectrum from the immediately preceding spectrum. Late in the time course, after the point at which the 394-nm absorbance began to increase, the 10-s-interval difference spectra all exhibited nearly identical shape. The difference spectrum designated "corrinoid component" was obtained by subtraction of two of the original spectra taken over a 20-s period during the time of maximal increase in absorbance at 394 nm. Difference spectral changes occurring in the early phase of the reaction (after the first 10-s interval) were somewhat variable in shape. The variation in shape resulted from increasing contributions of the corrinoid component, detected only after the initial 10-s interval. The standard "Fe/S component" difference spectrum was obtained from a separate reaction mixture that was identical except for the presence of 12 nmol of CH_3-H_4SPt by subtraction of two spectra taken 20 s apart early in the reaction during the period of maximal decrease in absorbance at 420 nm. In the absence of CH_3-H_4SPt, attempts to derive a difference spectral component reflecting changes that occur exclusively during the initial phase of reaction yielded a composite spectrum that was similar in shape to the Fe/S component standard, except for a slight shoulder around 394 nm (indicating unwanted contribution from the corrinoid component).

Corrinoid Redox Midpoint Potential. The redox state of the corrinoid component of the CODH–corrinoid enzyme complex was analyzed in solutions equilibrated with gas mixtures containing CO and CO_2 in various proportions.[2] The enzyme complex was added to solutions contained in a 1.5-mL semimicro spectrophotometer cuvette preequilibrated with the different gas mixtures. The solutions were prepared by adding 150 μL of 0.2 M sodium 2-(*N*-morpholino)ethanesulfonate (MES), pH 6.0, and the correct volume of stock 0.1 M sodium bicarbonate calculated to yield a pH of 6.0 under the partial pressures of CO_2 to be employed. After addition of water to a final volume of 540 μL, the gas mixture was bubbled through the solution for 12 min at a rate of approximately 15 cc/min using a 26-gauge syringe needle. A 40-μL sample of the enzyme (previously thawed under argon and protected from hydrogen present in the atmosphere of the anaerobic laboratory) was added to the cuvette after adjustment of the gas outlet to maintain a blanket of CO_2+CO gas mixture above the solution without further bubbling. Spectral data were recorded at 1-min intervals until no further changes were detected, approximately 12–15 min. Spectral changes occurred reversibly in both oxidative and reductive directions.

Potential measurements were conducted in separate experiments on solutions (600 μL) previously equilibrated by bubbling with CO_2+CO gas mixtures, containing the enzyme complex (0.8 μM corrinoid) in the presence of methyl viologen and TRIQUAT (approx. 40 μM each). A polished platinum wire was used with a Ag/AgCl reference electrode operating at a potential of 194 mV (−48 mV relative to a calomel electrode primary standard). Prior to addition of the enzyme, gas bubbling was stopped and the CO_2+CO gas mixture was allowed to flow over the solution with stirring until attainment of a stable potential .

Synthesis of Acetyl-CoA from CoASH, CO, and CH_3-H_4SPt. Synthesis of acetyl-CoA was monitored spectrophotometrically in 600-μL-volume reactions conducted in stoppered semimicro cuvettes inside the Anaerobic Laboratory. The assay was based on the difference in the molar absorptivity of the methyl group donor reactant CH_3-H_4SPt and the demethylated product H_4SPt, $\Delta\epsilon = 3600\ M^{-1}\ cm^{-1}$ (Grahame, 1991). Carbon monoxide saturated water, 200 μL, was added to 390 μL of an argon-saturated solution buffered at pH 7.2 with 30 μmol of MOPS and containing approximately 64 nmol of CH_3-H_4SPt and the enzyme complex (0.47 nmol of corrinoid). The cuvette was immediately stoppered and placed in the cell compartment of the spectrophotometer maintained at 36 °C. After temperature equilibration for 5 min, the reaction was initiated by addition of 10 μL of anaerobic 10 mM coenzyme A. Spectral recordings were begun prior to the start of the reaction and were continued throughout the reaction. The spectrum taken before the start of the reaction was multiplied by a factor of 0.9833 to correct for subsequent dilution and was modified below 300 nm by adding to it the spectrum of 0.167 mM coenzyme A, recorded separately. Difference spectra, developed during the time course of the reaction, were calculated by subtracting the modified initial spectrum from all other spectra subsequently recorded. Reversed-phase HPLC analysis of reaction products was conducted as described previously (Grahame, 1991).

RESULTS

UV-Visible Absorption Spectral Properties. Reactions of carbon monoxide with the *M. barkeri* CODH–corrinoid enzyme complex were investigated by UV-visible absorption spectroscopy. The absorption spectrum of the enzyme complex as isolated is shown in Figure 1 (dashed lines). The brown-colored preparation exhibited relatively strong absorbance in the visible region that consisted of a broad shoulder centered around 400 nm, with significant absorbance extending out to 800 nm and beyond. Features of the spectrum are consistent with the presence of Fe←S charge-transfer bands originating from Fe-S centers in the enzyme complex. Exposure of the enzyme to carbon monoxide caused marked bleaching of the Fe-S absorbance and, in addition, resulted in a sharp peak of increased absorbance at 394 nm, indicating the reduction of the enzyme-bound corrinoid cofactor to the Co^{1+} oxidation state. A relatively low molar excess of CO over enzyme corrinoid (approx. 7.4-fold) was sufficient for all changes detected in the spectrum to reach apparent completion.

Multicomponent Analysis of Redox Difference Spectra. At low concentrations of enzyme and carbon monoxide, reduction of the enzyme was sufficiently slow that spectral changes could be recorded during the progress of the reaction. Spectral changes at the beginning of the reaction with CO

[2] An apparatus was designed to mix gasses and subsequently deliver the gas mixture at a controlled rate. The device consisted of a tightly stoppered 500-mL glass aspirator bottle connected at the lower outlet by vinyl tubing to a reservoir held about 20–30 cm above the neck of the bottle. The stoppered bottle was filled completely with 0.1 N H_2SO_4 (to prevent absorption of CO_2) saturated with argon just before use. Different gases were added separately with a 60-cc syringe through the stopper (fitted with a gas-tight valve and female luer fitting), forming the head space in the aspirator bottle and causing displacement of the acid solution into the upper reservoir. Under the hydrostatic pressure of the upper reservoir, by way of a needle inserted through the stopper, the head space gas mixture was permitted to flow back out of the apparatus to reaction mixtures under study. Flow was initiated about 5 min after all gas additions were complete. Turbulence created by initial injection of the gases into the bottle appeared sufficient to cause adequate gas mixing since the order of gas addition and the final volume of the gas mixture had no effect on the measured potential or extent of reduction of the enzyme.

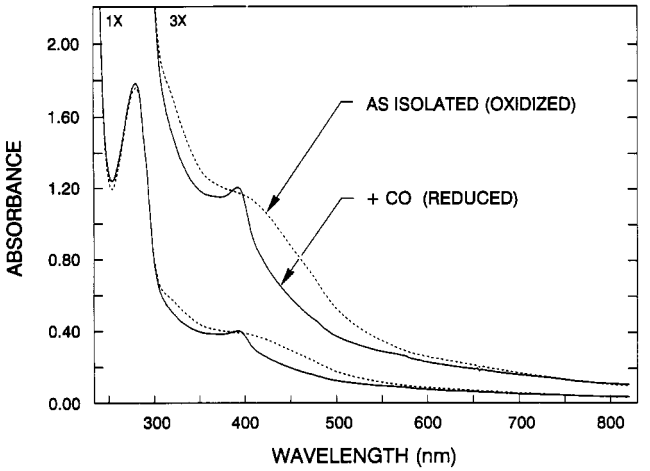

FIGURE 1: Effect of carbon monoxide on the electronic absorption spectrum of the CO oxidoreductase–corrinoid enzyme complex. The UV-visible absorption spectrum is shown of a sample of the enzyme complex (2.7 μM corrinoid) under 100% argon, purified as described under Materials and Methods (dashed line). The spectrum of the reduced enzyme complex is given (solid line), recorded upon completion of reaction with 20 μM carbon monoxide as described under Materials and Methods. In order to show better detail in the visible region, the raw data (1×) were replotted after multiplication by a factor of 3 (3×).

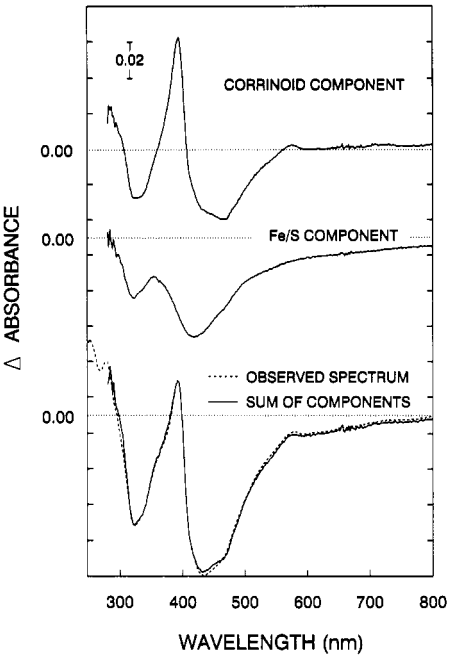

FIGURE 2: Two predominant spectral components forming the overall reduced-minus-oxidized difference spectrum of the CO oxidoreductase–corrinoid enzyme complex. The spectral change (final-minus-initial) produced after 2.7 min of reaction of the enzyme complex with carbon monoxide conducted as described in the caption to Figure 1 is shown in the bottom panel (dashed line, OBSERVED SPECTRUM). In the middle and upper panels are shown two independent difference spectral components designated Fe/S and CORRINOID, respectively. The component spectra were obtained, as described under Materials and Methods, from transient spectral changes observed during the progress of reduction of the enzyme complex. The corrinoid and Fe/S spectral components are shown with the same amplitudes used for optimal fit of the observed spectrum. As indicated under Materials and Methods, analysis of fit to the observed spectrum was performed, over the 300–650-nm region, by linear algebraic multicomponent analysis using a least squares criterion. The simulated spectrum shown in the bottom panel (solid line, SUM OF COMPONENTS) was obtained by direct summation of the Fe/S and corrinoid component spectra shown.

were characteristically different in shape from the spectral changes recorded near the end of the reaction.

A composite difference spectrum was calculated by subtraction of two spectra recorded over a short time interval during the initial phase of the reaction, as described under Materials and Methods. This composite difference spectrum (designated Fe/S COMPONENT in Figure 2) displayed a major region of maximal absorbance decrease at approximately 418 nm and a minor negative peak at about 322 nm. The composite spectrum was similar to difference spectra observed upon reduction of other proteins containing Fe-S clusters. For example, the reduced-minus-oxidized difference spectrum of *M. barkeri* ferredoxin exhibited major and minor negative peaks at approximately 420 and 318 nm, respectively.[3]

By analogous means, a difference spectrum was obtained representing the changes occurring in the final stages of the reaction. The difference spectrum (Figure 2, CORRINOID COMPONENT) showed a sharp, positive peak of increased absorbance at 394 nm, characteristic of formation of a reduced Co^{1+} corrinoid cofactor. The corrinoid component spectrum strongly resembled the overall shape of the Co^{1+}-minus-Co^{2+} difference spectrum of cobalamin.[4]

Sequential Reduction of Fe/S and Corrinoid Centers. Subtraction of the oxidized and CO-reduced spectra given in Figure 1 yielded a difference spectrum for overall reduction of the enzyme complex, as shown in Figure 2 (OBSERVED SPECTRUM). Multicomponent analyses with least squares fitting was used to match the overall reduced-minus-oxidized difference spectrum to a combination of the two standard components (corrinoid and Fe/S) summed independently according to Beer's law. As shown in Figure 2, summation of the best-fit quantities of the Fe/S and corrinoid components (Figure 2, SUM OF COMPONENTS) yielded a close approximation to the overall difference spectrum observed.

Multicomponent analyses were also carried out on a series of difference spectra obtained from data recorded throughout the progress of CO reduction of the enzyme complex. The results are plotted in Figure 3 as percent of each component obtained from the analysis (relative to the maximum amount found) versus time of the reaction. As shown in Figure 3, the time course of enzyme complex reduction was marked by sequential changes in the relative contributions of the Fe/S and corrinoid spectral components. The results indicated that reduction of redox centers in the enzyme complex occurs in a stepwise fashion: electrons derived from oxidation of CO enter initially into reduction of Fe-S centers and subsequently cause reduction of the corrinoid cofactor to the Co^{1+} state.

Reaction of the Co^{1+} Corrinoid with CH_3-H_4SPt. Addition of excess N^5-methyltetrahydrosarcinapterin to the reduced enzyme complex (approx. 7.4 mol of CH_3-H_4SPt/mol of enzyme corrinoid) caused immediate, and virtually complete, loss of the peak at 394 nm. The 394-nm peak was abolished (indicating loss of the Co^{1+} oxidation state) within the time required for mixing and subsequent recording of the spectrum (less than ~4 s). Loss of the Co^{1+} oxidation state suggested

[3] Data are from unpublished spectrophotometric analyses of the catalytic reduction of purified *M. barkeri* ferredoxin (Grahame, 1991) by hydrogenase in the presence of hydrogen.

[4] Literature spectra of cob(I)alamin and cob(II)alamin at equal concentrations (Dolphin, 1971) were digitized and subtracted for comparison with the corrinoid component difference spectrum. The cob(I)alamin-minus-cob(II)alamin difference spectrum showed a positive peak at 388 nm in comparison with the 394-nm peak of the corrinoid protein component (Figure 2, CORRINOID COMPONENT). Negative peaks (troughs) at approximately 332 and 477 nm corresponded to similar features in the corrinoid component spectrum at 328 and 468 nm (Figure 2, CORRINOID COMPONENT).

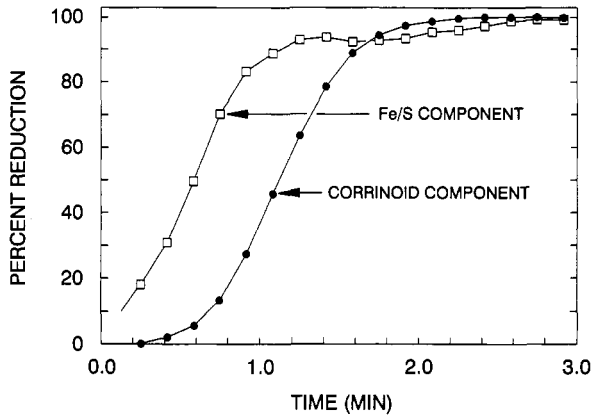

FIGURE 3: Sequential reduction of iron–sulfur and corrinoid centers revealed by time-dependent changes in redox difference spectra. Results from multicomponent analysis are plotted as a function of time of reaction with carbon monoxide in a reaction carried out under conditions described in the caption to Figure 1. Relative contributions of corrinoid and Fe/S components were determined by multicomponent analyses carried out on difference spectra (spectrum at t minus spectrum at t_0) obtained as a function of time of reaction. The contribution of each component is plotted as percent (PERCENT REDUCTION) of the maximum value obtained versus time.

formation of Co^{3+}-methyl corrinoid by methyl group transfer from CH_3-H_4SPt.

In a separate test, reaction of the nonreduced enzyme complex (as isolated, in the absence of reducing agents) was monitored after simultaneous addition of 20 μM carbon monoxide and 20 μM CH_3-H_4SPt. The reaction followed approximately the same initial time course as shown in Figure 3, with the exception that the Co^{1+} corrinoid component was never detected. These results confirmed that loss of the Co^{1+} oxidation state in the presence of CH_3-H_4SPt was almost certainly not due to inadvertent oxidation of the corrinoid. Although CO and CH_3-H_4SPt were present at equal concentrations, the reaction of CO with the enzyme required at least 40 times longer to reach apparent completion than the reaction of the reduced enzyme with CH_3-H_4SPt. This result demonstrated that methyl group transfer from CH_3-H_4SPt is fast relative to the rate of enzyme reduction by carbon monoxide.

In the presence of methyl iodide, the CO-reduced enzyme complex exhibited a slow loss of the peak at 394 nm, indicating sluggish methylation of the corrinoid. In contrast, there was no detectable influence on the Co^{1+} corrinoid spectrum by *S*-adenosylmethionine. The results indicated that transfer of the methyl group from CH_3-H_4SPt to the Co^{1+} corrinoid resulted in formation of H_4SPt and the Co^{3+}-methyl corrinoid. The specific requirement for CH_3-H_4SPt as methyl group donor further indicates that methyl group transfer may be enzyme-catalyzed.

Redox Midpoint Potential of the Corrinoid $Co^{2+/1+}$ Couple. Multicomponent analysis of difference absorption spectra was used to determine the relative extent of Co^{1+} corrinoid formation at different redox potentials. Control of redox potential using viologen dye mediators was impractical because accurate spectral deconvolution was prevented by strong interference of reduced viologens with the 394-nm reduced corrinoid peak. Instead it was found that redox potential could be controlled by equilibrating solutions containing the enzyme complex with gas atmosphere mixtures composed of carbon monoxide and carbon dioxide in fixed proportions. This technique predictably established the solution redox potential, measured at platinum in the presence of viologen dye mediators, as shown in Figure 4A. Stable potentials were

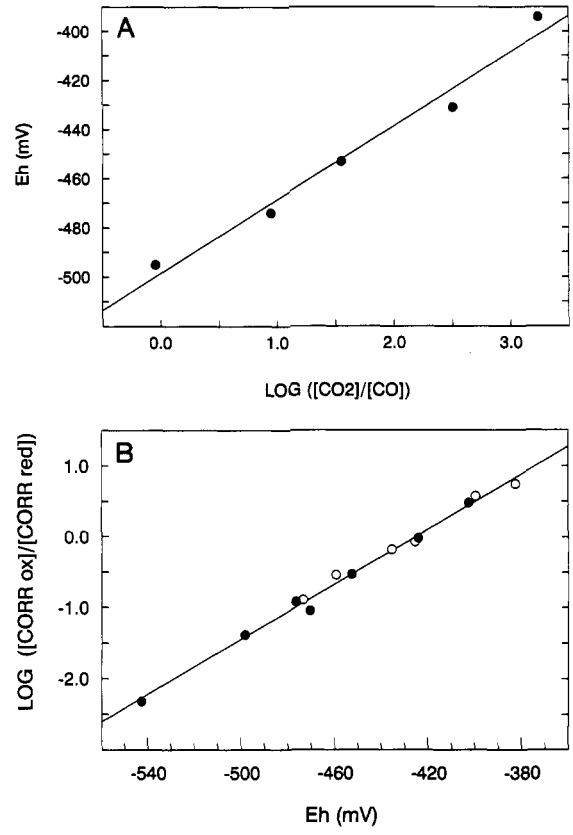

FIGURE 4: Corrinoid $Co^{2+/1+}$ redox midpoint potential determination. The extent of corrinoid reduction was measured spectrophotometrically in solutions containing the enzyme complex at pH 6.0 poised at potentials established by equilibration with CO_2/CO mixed gas atmospheres of fixed composition as described under Materials and Methods. Solution potential was calculated as $E_h = E_0 + 2.303 \times (RT/nF) \log([CO_2]/[CO])$. The numerical values of n ($n = 2.0$ equiv) and E_0 ($E_0 = -499$ mV) were determined from data obtained in separate experiments (described under Materials and Methods), wherein potentials established by the CO_2/CO couple were measured directly. The measured potentials are shown in panel A plotted versus $\log([CO_2]/[CO])$, according to the Nernst equation. The log of the oxidized corrinoid/reduced corrinoid concentration ratio, LOG ([CORR ox]/[CORR red]), was determined as described under Materials and Method and is plotted in panel B (filled symbols) as a function of the calculated potential. Additional data in panel B (open symbols) correspond to $\log([\text{corrinoid}_{ox}]/[\text{corrinoid}_{red}])$ values observed at potentials established under 100% hydrogen at pH values ranging from pH 6.4 to 8.0. Potentials fixed by the H^+/H_2 ratio were calculated as indicated under Results and were also verified experimentally.[4]

obtained less than 10 min after addition of the enzyme complex to solutions equilibrated with the gas mixtures. The results show that stable potentials were fixed by the $[CO_2]/[CO]$ concentration ratios according to the Nernst relationship, with a slope of 30.0 mV (n = 1.97 electron equiv) yielding an apparent midpoint potential of –499 mV for the CO_2/CO couple at pH 6.0 (Figure 4A).

In order to determine the corrinoid $Co^{2+/1+}$ redox midpoint potential, the absorption spectrum of the enzyme complex was recorded in solutions equilibrated with $[CO_2]/[CO]$ gas mixtures in the absence of viologen mediators, as described under Materials and Methods. The time periods required for spectral changes to reach apparent completion were similar to the periods required to establish stable potentials at platinum in the presence of viologen mediators. The spectrum of the enzyme complex recorded under 100% CO_2, in the absence of CO, was virtually identical in shape to the spectrum recorded under 100% argon (Figure 1, dashed lines). Under these conditions the enzyme complex was considered to contain the

corrinoid cofactor in the oxidized state. A difference spectral parameter, sensitive only to the extent of reduction of the corrinoid component, was used to calculate the oxidized corrinoid/reduced corrinoid ratio at different redox potentials. The parameter was obtained from the calculated reduced-minus-oxidized difference spectra by taking the difference in absorbance at 392 nm from absorbance at 430 nm corrected for the (dA_{392}–dA_{430}) contributed by Fe/S component absorbance determined from multicomponent analysis. The oxidized corrinoid/reduced corrinoid ratio was calculated from the spectral parameter after assigning the value of 100% reduction equal to the maximum parameter observed, multiplied by 1.005. The results, analyzed according to the Nernst equation, are shown in Figure 4B (closed symbols) plotted as $\log_{10}([\text{corrinoid}_{ox}]/[\text{corrinoid}_{red}])$ versus potential (NHE). From ordinary least squares regression analysis of the data the corrinoid $Co^{2+/1+}$ redox midpoint potential was found to be –426 mV (±4 mV) at pH 6.0 and 24 °C. The slope of the plotted line was 1/51.0 mV^{-1}, indicating that reduction of the corrinoid proceeded by a one-electron process (n = 1.16 electron equiv).

A second experiment was conducted to measure the corrinoid $Co^{2+/1+}$ midpoint potential using a different approach for poising the redox potential not dependent on reaction with CO_2 or CO. The method takes advantage of a low level of hydrogenase activity indicated to be present in the enzyme complex preparation by the following spectrophotometric observations: (1) Incubation under H_2 caused the enzyme Fe-S and corrinoid centers to become reduced. (2) Reoxidation of the H_2-reduced enzyme followed after the gas phase was replaced with 100% argon. Variation of the redox potential was achieved by equilibrating solutions of the enzyme complex with 100% hydrogen gas at various pH values in the range pH 6.4–8.0. During equilibration, spectra were recorded as a function of time. The results indicated that at least 30 min was required for apparent completion of the reaction at high pH, whereas under conditions of low pH more than 80 min of incubation was needed for cessation of further changes in the spectra. In reactions at different pH values, the potential E_h was determined on the basis of the pH dependence of the H^+/H_2 couple (with E_0 = 0.0 mV), given that $E_h = E_0 - (\text{pH})2.303(RT/F)$. Spectrophotometric evidence was obtained indicating that this procedure accurately establishes the solution potentials calculated.[5]

Data from hydrogenase reduction of the enzyme complex at various potentials fixed by the H^+/H_2 couple were obtained from multicomponent analyses of redox difference spectra, as before. Analysis of the H^+/H_2 data (open symbols in Figure 4B) according to the Nernst equation using ordinary least squares regression yielded a value of the corrinoid $Co^{2+/1+}$ midpoint potential that was identical within experimental error to the value obtained by the method using CO_2/CO gas mixtures. Since the results were found to obey the Nernst equation closely, the corrinoid $Co^{2+/1+}$ midpoint potential appears to be independent of pH within the region tested.

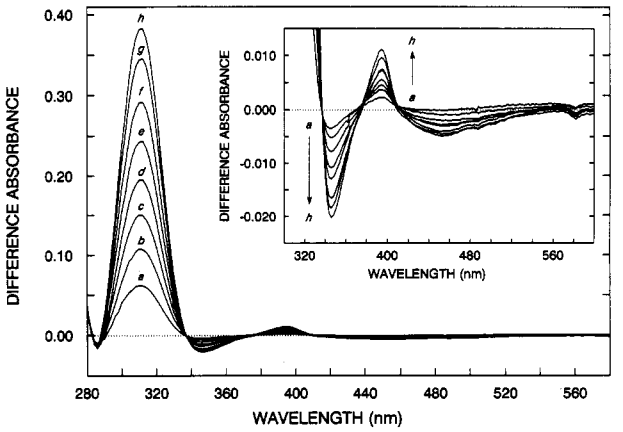

FIGURE 5: Synthesis of acetyl-CoA and regeneration of the Co^{1+} corrinoid intermediate during demethylation and consumption of CH_3-H_4SPt. Conditions for synthesis of acetyl-CoA at 36 °C from coenzyme A, CO, and CH_3-H_4SPt were as described under Materials and Methods. Difference spectra, calculated by subtraction of the zero-time spectrum as indicated under Materials and Methods, were obtained after reaction time periods of (*a*) 0.58, (*b*) 2.58, (*c*) 4.58, (*d*) 6.58, (*e*) 8.58, (*f*) 10.58, (*g*) 12.58, and (*h*) 14.08 min. In the wavelength region around 330–560 nm, difference spectra are shown replotted on an enlarged scale (inset).

The solid line drawn in Figure 4B shows the results of regression analysis on the data combined from both experiments. Analysis of both data sets together yielded a value for the corrinoid $Co^{2+/1+}$ redox midpoint potential of –426 mV (±4 mV). The slope of the line was 1/51.8 mV^{-1}, indicating, as before, that the observed spectral changes represent one-electron reduction of the corrinoid (n = 1.14 electron equiv).

Net Synthesis of Acetyl-CoA from CoASH, CO, and CH_3H_4SPt. In a spectrophotometer cuvette under argon approximately 9.9 nmol of CO (10 μL of CO-saturated water) was added to a mixture (590 μL) of the enzyme complex (1.9 nmol of corrinoid) and a moderate excess of CH_3-H_4SPt (approx. 5 nmol). As noted earlier, a distinct peak in the absorption spectrum of the reduced enzyme complex at 394 nm was not observed in the presence of CH_3-H_4SPt. However, a prominent peak at 394 nm appeared rapidly upon addition of coenzyme A (approx. 24 nmol) to the mixture. This observation suggested that demethylation of the Co^{3+}-methyl corrinoid had occurred, producing the Co^{1+} corrinoid by a reaction dependent on coenzyme A. Furthermore, it was postulated that residual CH_3-H_4SPt was turned over in the process and consumed; otherwise, remethylation of the Co^{1+} corrinoid would have prevented formation of the 394-nm peak.

In order to test whether CH_3-H_4SPt was undergoing turnover, reactions were set up containing much larger quantities of CH_3-H_4SPt. A reaction in a mixture containing approximately 64 nmol of CH_3-H_4SPt, 200 nmol of CO, and enzyme complex (0.47 nmol of corrinoid) was initiated by addition of 100 nmol of CoASH and monitored spectrophotometrically. As shown in Figure 5, spectral changes over time resulted in a prominent peak of increased absorbance at 312 nm. The 312-nm peak was virtually identical, but opposite in sign, to the major spectral change that occurs due to methylation of H_4SPt to form CH_3-H_4SPt during overall cleavage of acetyl-CoA [Figure 4B in Grahame (1991)]. Therefore, these results indicate extensive consumption and turnover of CH_3-H_4SPt with concomitant production of the demethylated product H_4SPt.

[5] The extent of reduction of *M. barkeri* ferredoxin was determined at pH 6.00, 7.22, and 7.78 in reaction mixtures saturated with hydrogen at 1 atm and containing sufficiently low levels of the enzyme complex preparation to avoid significant spectral interference. From the observed extent of reduction and the midpoint potential of the ferredoxin, determined voltammetrically to be –420 mV at pH 8.0 (Grahame, 1991), apparent values of E_h were calculated at the pH values indicated. The E_h values so obtained were close to the potentials calculated on the basis of the pH dependence of the H^+/H_2 couple. In addition, the redox midpoint potential of ferredoxin was not found to be strongly affected by pH in the range of the experiment. The results indicate that potentials calculated on the basis of the H^+/H_2 couple pH dependence very likely reflect the actual potentials imposed.

Analyses of the reaction products by reversed-phase HPLC (not shown) confirmed that CH_3-H_4SPt had been converted to H_4SPt and, in addition, provided direct evidence for depletion of CoASH and production of acetyl-CoA. Quantitative HPLC analyses were performed on the products from several different reactions at completion containing different limiting quantities of CH_3-H_4SPt. The results showed that production of acetyl-CoA was stoichiometric with the consumption of CH_3-H_4SPt. Under the conditions shown in Figure 5, the rate of acetyl-CoA synthesis was 31 nmol/min/mg of protein. This is approximately 1.6 times higher than the initial rate of cleavage of acetyl-CoA observed earlier (Grahame, 1991). In contrast to the cleavage reaction, the acetyl-CoA synthesis rate does not decline as the reaction proceeds, as indicated by the data shown in Figure 5. A sharp bend to 0 slope occurred in plots of A_{312nm} versus time at the point when substrate CH_3-H_4SPt was consumed (data not shown).

In addition to the major spectral changes produced by conversion of the substrate CH_3-H_4SPt to product H_4SPt, minor features were also detected that could be attributed to changes occurring on the enzyme complex itself. These features, shown in the inset to Figure 5, consisted of a sharp peak of increased absorbance at 394 nm and a broad band of decreased absorbance centered at 452 nm. The increase at 394 nm indicated that Co^{1+} corrinoid was regenerated during the course of the reaction. Loss of absorbance at 452 nm is consistent with demethylation of base off Co^{3+}-methyl corrinoid. Three fairly well-defined isosbestic points were observed. The first, at 337 nm, appears to result from CH_3-H_4SPt/H_4SPt conversion. The other two isosbestic points were observed in a region where there is no absorption by H_4SPt or CH_3-H_4SPt. The occurrence of these two isosbestic points, at 376 and 410 nm, constitutes evidence that the 394-nm Co^{1+} corrinoid peak is regenerated from the species absorbing at 452 nm without formation of a detectable intermediate state.

DISCUSSION

Substrate and cofactor reactivity of the acetyl-CoA-cleaving multienzyme complex from *M. barkeri* was studied using UV-visible spectroscopy. In reactions using coenzyme A, CH_3-H_4SPt, and carbon monoxide, the enzyme complex functions efficiently in synthesis of acetyl-CoA. As demonstrated by the results from spectrophotometric and HPLC analyses, acetyl-CoA was rapidly and steadily synthesized by a reaction highly analogous to the reverse of eq 1. Quantitative data indicate the stoichiometry shown in the following balanced equation.

$$CH_3\text{-}H_4SPt + CO + CoASH \rightarrow CH_3CO\text{-}SCoA + H_4SPt \quad (2)$$

By addition of the CO_2/CO redox equivalence (eq 3), eq 2 can be considered to be formally identical to the reverse of eq 1.

$$CO_2 + 2H^+ + 2e^- \rightleftharpoons CO + H_2O \quad (3)$$

The reduced Co^{1+} state of the corrinoid is readily detected in the CO-reduced enzyme complex by the absorption peak at 394 nm. The Co^{1+} corrinoid is rapidly methylated upon addition of CH_3-H_4SPt, as indicated by the virtually instantaneous loss of the peak at 394 nm. Further evidence for methyl group transfer is provided by the spectral changes that occur during the progress of acetyl-CoA synthesis (eq 2). Regeneration of the enzyme Co^{1+} corrinoid is observed concomitant with the conversion of CH_3-H_4SPt to H_4SPt. The data are consistent with rapid methyl group transfer between pterin and corrinoid components in an equilibrium process, as shown in the following equation.

$$Co(I)corrinoid + CH_3\text{-}H_4SPt + H^+ \overset{FAST}{\rightleftharpoons} CH_3\text{-}Co(III)corrinoid + H_4SPt \quad (4)$$

Methyl group transfer (eq 4) appears to be exceedingly fast since the rate of methylation of the Co^{1+} corrinoid was too rapid to measure by the techniques employed. In contrast, reaction of the enzyme complex with low concentrations of carbon monoxide proceeds at a rate that can be followed by standard UV-visible spectroscopy. The rate of acetyl-CoA synthesis did not decrease as the concentration of CH_3-H_4SPt and the Co^{3+}-methyl corrinoid declined, indicating that methyl group donation does not limit the rate of acetyl-CoA synthesis under the conditions employed. The results allow speculation that other steps, such as C–C bond formation, may be rate limiting in overall acetyl-CoA synthesis and cleavage.

Reaction with carbon monoxide results in sequential changes in the shape of the absorption spectrum of the enzyme complex. Analysis of the CO-reduced-minus-oxidized difference spectra reveals two major components. Overall difference spectra observed throughout the reaction are reasonably well fit by linear combinations of the two independent spectral components. The predominant spectral component late in the reaction (Figure 3, CORRINOID COMPONENT) corresponds to reduction of the corrinoid cofactor to the Co^{1+} oxidation state. The major component observed early in the reaction (Figure 3, Fe/S COMPONENT) is ascribed to general iron–sulfur center reduction. The exact number of iron atoms involved, and the structures of the Fe-S clusters, have not been established. However, using a difference extinction coefficient at 420 nm of 1900 M^{-1} cm^{-1} per atom of iron,[6] it may be estimated roughly that 12 Fe atoms (per corrinoid) contribute to the Fe/S component spectrum.

In solutions containing CO_2 and CO, the redox state of the corrinoid cofactor varies depending on the CO_2/CO ratio. Measurements made with a platinum electrode in mixtures containing the CODH–corrinoid complex and viologen mediators establish that the redox potential is effectively poised by the ratio of CO_2 to CO according to the Nernst equation in a two-electron process of midpoint potential –499 mV (eq 3) at pH 6.0. In the absence of exogenous mediators, half-reduction of the corrinoid occurs at a potential of –426 mV. Corrinoid redox changes obey the Nernst equation as a one-electron process. Changes in the redox state of the corrinoid mediated by hydrogenase under an atmosphere of hydrogen are in agreement with a midpoint potential of –426 mV. In addition, the corrinoid midpoint potential is independent of pH in the range tested, pH 6.4 to 8.0. Since reduction to the Co^{1+} level occurred as a one-electron process, the isolated enzyme most likely contained the Co^{2+} form of the cofactor. The corrinoid redox process can be written as follows.

$$Co^{2+}\text{-corrinoid} + 1e^- \rightleftharpoons Co^{1+}\text{-corrinoid}, \quad E_0' = -426\ mV \quad (5)$$

General changes in the redox state of Fe-S centers, as monitored by the Fe/S spectral component contribution, were

[6] A $\Delta\epsilon_{420nm}$ value of 1900 $M^{-1}cm^{-1}$ was obtained from the value of ϵ_{400nm} = 4000 M^{-1} cm^{-1} per iron in $[4Fe\text{-}4S]^{2+}$ centers (Sweeney & Rabinowitz, 1980) after the lower absorbance at 420 than at 400 nm and the expected 50% decrease in absorbance at 420 nm upon reduction were accounted for (Sweeney & Rabinowitz, 1980).

virtually complete at potentials below about –420 mV. At the least negative potential tested (–383 mV, pH 6.4), approximately 70% of the Fe/S spectral component change had already occurred. The data illustrating sequential time-dependent reduction of Fe-S and corrinoid centers, shown in Figure 3, are consistent with a reaction scheme involving rapid, reversible electron transfer between corrinoid and Fe-S redox centers differing in redox midpoint potential by approximately 80 mV. If redox equilibrium between the corrinoid cofactor and Fe-S centers is attained much faster than the rate of CO reduction of the enzyme, then the redox state of the corrinoid will be related approximately to that of the Fe-S center(s) at any given time according to the expression for two combined $1e^-$ half-reactions, $E_{mcorr} - E_{mFe\text{-}S} = \Delta E_m = (2.303RT/nF) \log([Fe\text{-}S_{ox}][corr_{red}]/[Fe\text{-}S_{red}][corr_{ox}])$. Data from Figure 3 in the range 0.4–1.1 min were used to solve the above expression and yielded a ΔE_m of –80 mV (±3mV SD for five points). These data suggest that the *apparent* rate of corrinoid reduction may be limited by the rate of CO reduction of a specific Fe-S center(s), that in turn may serve as immediate electron donor to the corrinoid cofactor.

At neutral pH, aquocobalamin exists in solution as the base-on form with $Co^{2+/1+}$ midpoint potential about –609 mV (Lexa & Saveant, 1976). At lower pH, the base-off configuration predominates and the redox potential is shifted to –500 mV. Protein-bound, base-off corrinoid cofactors are also reported with $Co^{2+/1+}$ midpoint potentials around –504 mV, in the case of the corrinoid/iron–sulfur protein from an acetogenic organism (Harder et al., 1989), and –486 mV for an analogous protein from a methanogen (Jablonski et al., 1993). However, base-on cobalamin in *Escherichia coli* methionine synthase exhibits a value (–526 mV) for the $Co^{2+/1+}$ midpoint potential that is less negative than the base-off form (–572 mV) (Banerjee et al., 1990). Therefore, the effect of coordination of the α-axial ligand cannot be the only factor that modulates the $Co^{2+/1+}$ redox potential of cobalamin and cobamide derivatives bound to proteins (Banerjee & Matthews, 1990).

Methyl group transfer from *S*-adenosylmethionine (AdoMet) to methionine synthase-bound cob(I)alamin is highly exergonic and substantially more favorable than methyl group transfer from N^5-methyltetrahydrofolate (CH_3-H_4folate). Thus, it appears that the reduced Co^{1+} corrinoid enzyme complex from *M. barkeri* fails to react with AdoMet for kinetic reasons rather than on thermodynamic grounds. In methionine synthase the presence of CH_3-H_4folate renders a difficult reduction to the Co^{1+} state somewhat less unfavorable, causing a significant shift of the cobalamin $Co^{2+/1+}$ apparent midpoint potential from –526 to around –450 mV (Banerjee et al., 1990). However, *S*-adenosylmethionine, a much more potent methylating agent than CH_3-H_4folate, is thought to reactivate the inactive, predominantly Co^{2+} state of the enzyme by trapping low equilibrium concentrations of the Co^{1+} form. In comparison, CH_3-H_4SPt, a compound of chemical methylating potential similar to CH_3-H_4folate, is highly effective in trapping the Co^{1+} corrinoid formed during the course of reduction of the *M. barkeri* enzyme complex. Efficient trapping by CH_3-H_4SPt may result since the $Co^{2+/1+}$ midpoint potential is fully 101 mV less negative than in methionine synthase. With an equilibrium ratio Co^{1+}/Co^{2+} 50 times higher than in methionine synthase, up to 50 times higher relative concentrations of the reactive Co^{1+} corrinoid may be available for methylation.

The $Co^{2+/1+}$ redox midpoint potential values reported for other corrinoid enzymes and proteins are significantly more negative than found here for the *M. barkeri* CODH–corrinoid enzyme complex. This implies that the reactive corrinoid Co^{1+} redox state in the *M. barkeri* complex is substantially more accessible under physiological conditions than might otherwise have been considered.

ACKNOWLEDGMENT

Many of these experiments were performed while the author was working in the laboratory of Dr. Thressa C. Stadtman at the NIH National Heart, Lung, and Blood Institute. I am very grateful for her suggestions, enthusiasm, and support of research on methanogenesis. I am also especially thankful to Dr. J. Michael Poston for helpful discussions and expert assistance on many occasions in operation of the NIH Anaerobic Laboratory.

REFERENCES

Banerjee, R. V., & Matthews, R. G. (1990) *FASEB J. 4*, 1450–1459.
Banerjee, R. V., Harder, S. R., Ragsdale, S. W., & Matthews, R. G. (1990) *Biochemistry 29*, 1129–1135.
Bradford, M. M. (1976) *Anal. Biochem. 72*, 248–254.
Dolphin, D. (1971) *Methods Enzymol. 18C*, 34–52.
Ferry, J. G. (1992a) *J. Bacteriol. 174*, 5489–5495.
Ferry, J. G. (1992b) *Crit. Rev. Biochem. Mol. Biol. 27*, 473–503.
Fischer, R., & Thauer, R. K. (1990) *Arch. Microbiol. 153*, 156–162.
Grahame, D. A. (1991) *J. Biol. Chem. 266*, 22227–22233.
Grahame, D. A., & Stadtman, T. C. (1987) *J. Biol. Chem. 262*, 3706–3712.
Harder, S. R., Lu, W.-P., Feinberg, B. A., & Ragsdale, S. W. (1989) *Biochemistry 28*, 9080–9087.
Hu, S.-I., Drake, H. L., & Wood, H. G. (1982) *J. Bacteriol. 149*, 440–448.
Jablonski, P. E., Lu, W.-P., Ragsdale, S. W., & Ferry, J. G. (1993) *J. Biol. Chem. 268*, 325–329.
Lange, N. A., Ed. (1961) *Handbook of Chemistry*, 10th ed., pp 1091–1093, McGraw-Hill, New York.
Lexa, D., & Saveant, J. M. (1976) *J. Am. Chem. Soc. 98*, 2652–2658.
Lu, W.-P., Harder, S. R., & Ragsdale, S. W. (1990) *J. Biol. Chem. 265*, 3124–3133.
Pezacka, E., & Wood, H. G. (1986) *J. Biol. Chem. 261*, 1609–1615.
Pezacka, E., & Wood, H. G. (1988) *J. Biol. Chem. 263*, 16000–16006.
Poston, J. M., Stadtman, T. C., & Stadtman, E. R. (1971) *Methods Enzymol. 22*, 49–54.
Ragsdale, S. W., & Wood, H. G. (1985) *J. Biol. Chem. 260*, 3970–3977.
Ragsdale, S. W., Lindahl, P. A., & Münck, E. (1987) *J. Biol. Chem. 262*, 14289–14297.
Raybuck, S. A., Ramer, S. E., Abbanat, D. R., Peters, J. W., Orme-Johnson, W. H., Ferry, J. G., & Walsh, C. T. (1991) *J. Bacteriol. 173*, 929–932.
Roberts, J. R., Lu, W.-P. & Ragsdale, S. W. (1992) *J. Bacteriol. 174*, 4667–4676.
Sweeney, W. V., & Rabinowitz, J. C. (1980) *Annu. Rev. Biochem. 49*, 139–161.
Terlesky, K. C., Nelson, M. J., & Ferry, J. G. (1986) *J. Bacteriol. 168*, 1053–1058.